Sensors and Actuators B 139 (2009) 505–510

Contents lists available at ScienceDirect

Sensors and Actuators B: Chemical

journal homepage: www.elsevier.com/locate/snb

Evanescent-wave cavity ring-down detection of cytochrome *c* on surface-modified prisms

L. van der Sneppen[1], C. Gooijer, W. Ubachs, F. Ariese*

Laser Centre, Vrije Universiteit, De Boelelaan 1081-1083, 1081 HV Amsterdam, The Netherlands

ARTICLE INFO

Article history:
Received 9 December 2008
Received in revised form 13 March 2009
Accepted 20 March 2009
Available online 31 March 2009

Keywords:
Surface analysis
Liquid-phase CRDS
Surface modification
Absorption detection
Laser spectroscopy

ABSTRACT

Adsorption kinetics and molecular interactions on different surface interfaces are studied by means of evanescent-wave cavity ring-down spectroscopy, using total internal reflection surfaces onto which different self-assembled monolayers are covalently attached. The adsorption of cytochrome *c* (a positively charged, spherical heme protein) to a negatively charged bare silica surface, as well as to C_{18}-coated (hydrophobic) and C_3NH_2-coated (positively charged) silica have been studied. It is experimentally verified that these surface layers do not interfere with the sensitive measurement of adsorbed cyt *c* monolayers using the evanescent wave in a ring-down scheme. Attaching monolayers covalently to the silica total internal reflection surface is a first step towards the development of a biosensor that makes use of immobilized biomolecules for specific detection of analytes in solution.

1. Introduction

Cavity ring-down spectroscopy is a sensitive mode of absorption spectroscopy that is based on the rate of decay of light measured behind (at the exit port of) an optically stable cavity. This decay rate depends on reflection and scattering losses in the cavity; the additional presence of an absorber in the cavity will increase these losses and can thus be detected. In evanescent-wave cavity ring-down spectroscopy (EW-CRDS) [1], one of the reflections in the cavity is a total internal reflection (TIR) event. Only the (exponentially decaying, i.e., in the spatial domain) evanescent wave associated with this TIR event is being used for absorbance measurements. Since the penetration depth of the evanescent wave is on the order of a wavelength, only molecules adsorbed at or near the surface are being probed. In contrast to other TIR techniques such as EW-fluoroimmunoassays [2,3] or waveguide spectroscopy [4], EW-CRDS is spatially localized: a small sample volume is repeatedly probed. This permits miniaturization of the flow cell while maintaining an excellent sensitivity due to the multi-pass character of the measurement.

Techniques that are commonly used for studying adsorption kinetics of cytochrome *c* (cyt *c*) to surfaces include electrochemistry [5] and surface-enhanced resonance Raman spectroscopy [6]. However, these techniques are not quantitative or are only capable of detecting the molecules in the first monolayer on the surface. A strong feature of EW-CRDS, as with attenuated total reflectance (ATR) measurements, is the capability of measuring only molecules near the surface, and with a proper correction for bulk absorbance, also the molecules adsorbed in multiple layers on top of the first monolayer are detected. Several studies have been described involving cyt *c* adsorption to silica surfaces using ATR or waveguide absorption techniques [4,7–11]. Some of these studies involve the cyt *c* adsorption to surface-modified silica [7,9,10]. Unlike single-pass internal reflection spectroscopy, EW-CRDS is very sensitive due to its multi-pass character, while maintaining a small probing volume. EW-CRDS is therefore suitable for small-volume time-dependent studies (since the signal does not have to be integrated over a long time-span).

In a previous paper we have explored the possibility of using EW-CRDS as a detection technique in dynamic flow systems [12]. However, a crucial point regarding its potential as a detection system is the question whether modification of the TIR surface is possible without significantly affecting its total reflection qualities. This is the objective of the present study. We will show that self-assembled monolayers made in a one-step reaction from commercially available reagents provide a fast and user-friendly means of surface modification.

2. Experimental section

The set-up (see Fig. 1) is similar to the one used in a previous study [12]. Briefly, a cavity was constructed using mirrors

* Corresponding author. Tel.: +31 20 5987524; fax: +31 20 5987543.
E-mail address: ariese@few.vu.nl (F. Ariese).
[1] Current address: Physical and Theoretical Chemistry Laboratory, University of Oxford, Oxford, United Kingdom.

0925-4005/$ – see front matter © 2009 Elsevier B.V. All rights reserved.
doi:10.1016/j.snb.2009.03.048

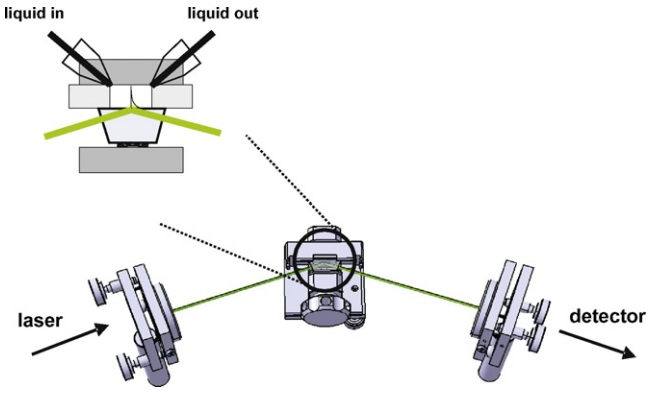

Fig. 1. The cavity with the 70° prism inserted. The prism is clamped on a platform that permits tilting in two directions as well as rotation of the prism; the platform is mounted on an *x*, *z* table. The insert shows the flow cell where the analyte solution is brought in contact with the TIR surface and is probed by the EW.

($R \geq 99.996\%$ at 532 nm, 50 mm radius of curvature) from REO Inc. (Boulder, CO, USA). Instead of the previously used 45° anti-reflection coated prism, a 70° Dove prism is used at normal incidence. The additional reflection losses at the intra-cavity surfaces are maintained in an embedded cavity [13]. The entrance and exit faces are polished to a flatness of $\lambda/10$ at 632.8 nm while the TIR face is polished to a flatness of $\lambda/2$. The rationale behind this modification is that the ring-down time of the cavity decreased from 1–1.5 μs to 20–25 ns upon inserting the 45° prism suggesting that there is room for improvement: new designs with lower reflection losses will provide increased sensitivity. Previously, we found that superpolishing of the TIR face to a surface roughness of only 0.2 nm did not improve the ring-down time but worked counterproductive for the observed signal [12]. With both the coated and the uncoated 70° prism, obtainable ring-down times were between 45 and 65 ns; they decreased to 30–45 ns for the highest concentrations of absorber used in this study. These ring-down times are still limited by the scatter and diffraction losses at the normal incidence surfaces on the prism, and not by the properties of the EW-surface nor by the mirror reflectivity. Another advantage of using a normal-incidence geometry for the entrance and the exit faces of the prism, rather than the previously used 45° anti-reflection coated prism, is that it permits for polarization-dependent studies. Although this advantage has not been exploited in the present study, measurement of the dichroic ratio can be used for determining the average molecular alignment of molecules in self-assembled thin films [14,15].

Laser pulses from an optical parametric oscillator (OPO), pumped with the 3rd harmonic of a Coherent Infinity single-mode Nd:YAG laser (Santa Clara, CA, USA), at a wavelength of 538 nm (the optimum of one of the two Q-transitions in the absorbance spectrum of cyt *c*) were used to excite the cavity at a repetition rate of 100 Hz. The wavelength used is close to the design wavelength for which the mirror coatings were produced. A moving average of 1 s or 100 data points was applied after fitting of the raw data. Transients were recorded using a photomultiplier tube (Hamamatsu, Shimokanzo, Japan) and a fast sampling oscilloscope of 1 GHz analog bandwidth (Tektronix 5104; 5 GS/s).

The baseline noise of the system is typically between 3 and 5×10^{-5} AU, an improvement over the set-up previously used (employing an anti-reflection coated 45° Dove prism in a linear cavity) which showed a baseline noise on the order of 10^{-4} AU [12].

Covalently bound monolayers were deposited on the TIR faces of the prisms according to a standard protocol for self-assembly from solution. Before the surface modifications, the prisms were thoroughly cleaned using chromic mixture ($K_2Cr_2O_7$ in H_2SO_4) followed by rinsing with abundant water. In order to obtain a uniform deposition of a silane monolayer, the surface was fully hydroxylated according to [16]: the prisms were immersed for 30 min in 1:1 (v/v) methanol:water followed by 30 min of immersion in 96% H_2SO_4. For the C_{18}-coating, trichloro-octadecylsilane (≥ 90%, Sigma–Aldrich, Germany) was used as a reagent. This reagent is very reactive towards water and should be handled in an anhydrous environment (e.g. N_2-filled glove-box). The reaction is completed by immersion of the TIR-face of the prism for 6 h in a solution of 20 μl of trichloro-octadecylsilane in 20 ml of toluene [17]. It should be emphasized that traces of water are appropriate since they accelerate the hydrolysis reaction. That is why the toluene (obtained from Riedel-de-Haen, Germany, containing 0.05% of water) was not dried prior to the reaction [18]. After the reaction, the prism was carefully cleaned and subsequently flushed with chloroform for 24 h. For the NH_2-coating, after the cleaning and hydroxylation steps, the prism was immersed for 5 min in methanol. Subsequently, the TIR face of the prism was immersed for 15 min in an aqueous solution (1%, v/v) of triethoxy-aminopropylsilane (≥ 90%, Sigma–Aldrich, Germany) followed by 5 min of ultrasonic cleaning in methanol and rinsing with abundant water [19]. Completion of the self-assembled layers was roughly estimated by monitoring the contact angle between a drop of water and the surface. Whereas the contact angle on a hydroxylated surface is 0°, the hydrophobic surfaces will yield a contact angle that is considerably larger. The coatings could be removed by leaving the prisms for several days in an abundance of chromic mixture.

The composition of the top surface after treatment was studied by XPS. Monochromatic Al K_α X-ray radiation was used to investigate the top 10 nm. Compositional information can be obtained from the element specific binding energies. Furthermore, limited in-depth information can be extracted from the intensity ratios. For quantification XPS sensitivity factors from the Scofield library [20] were used. In order to be able to accurately analyze composition, substrate charging was prevented by using silicon wafers instead of quartz prisms. Measurement of a treated prism and overlapping the oxygen signals to charge compensate, showed that a similarly treated Si wafer has the same top layer composition as the prism.

An XPS analysis of the clean and treated silicon wafer samples (see Fig. 2) shows that after treatment and transport through atmosphere, the elements oxygen (O 1s), carbon (C 1s) and silicon (Si 2s, Si 2p) are identified on all samples. Only the NH_2-coated sample shows a trace of nitrogen (N 1s) accounting for approximately 2% atomic concentration of the sampled volume. The C_{18}-treated sample has the largest C 1s peak, accounting for approximately 50% atomic concentration, whereas the amount of carbon present on the silica accounts for 10% atomic concentration (and somewhat higher

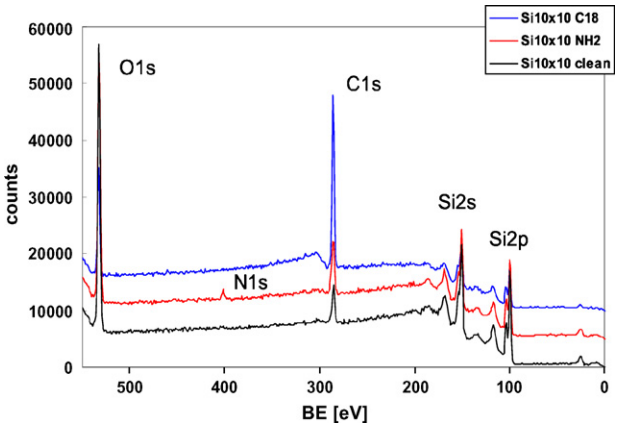

Fig. 2. XPS survey of differently treated 10 mm × 10 mm Si wafers. The elements oxygen (O 1s), nitrogen (N 1s), carbon (C 1s) and silicon (Si 2s, Si 2p) are identified.

for the NH_2-treated surface). It can be estimated from the XPS analysis that a 100%-coverage was obtained for the C_{18}-coated surface. The layer thickness on the C_{18}-modified wafer was measured to be on the order of 3–5 nm, which corresponds to a monolayer with fully stretched C_{18} chains [17]. Chlorine was not detected in the XPS surveys indicating that the reaction was complete. The NH_2-layer was immobilized using a different approach based on the less reactive triethoxysilane rather than trichlorosilane. The estimated monolayer coverage is only 50–75%.

The relatively small protein cytochrome *c* is often used as a benchmark molecule; the extinction coefficient was determined to be 1.0×10^4 $M^{-1}\,cm^{-1}$ at 538 nm by measurement of the absorbance spectrum of a 100 μM solution of cyt *c* on a Varian UV–Vis Cary 50 absorbance spectrometer. Cyt *c* has a net positive charge at a pH of 7.4 and is assumed to be spherical with a diameter of 3.0–3.5 nm [21]. Cytochrome *c* adsorption experiments are performed using a stopped-flow approach: 100 μl of a cyt *c* solution in 10 mM of potassium phosphate buffer at pH 7.4 is injected in a continuous flow (0.1 ml/min) of the same buffer. When the injection plug reaches the 14 μl-sized teflon flow cell, that is clamped leak-tight on the TIR face of the prism, the flow is stopped. The evolution of the absorbance signal is monitored for a period of 10–15 min. No degradation of the absorbance signal is observed after prolonged time-spans, it is therefore assumed that photodegradation of cyt *c* is negligible.

3. Results and discussion

3.1. Cytochrome c adsorption to bare silica

First of all we explored the performance of the system before chemical modification of the TIR surface. A typical flow profile of a stopped-flow experiment is shown in Fig. 3: immediately after stopping the flow, the absorbance (measured by CRDS) increases to a constant level. Starting the flow again leads leads to a gradual desorption and a slowly decreasing absorbance. After performing the experiments, silica surfaces were cleaned by overnight reaction in chromic mixture. Later an alternative cleaning method was found: a 100 μl injection of 0.1 M H_2SO_4 in a flow of 0.05 ml/min also desorbs the cyt *c* completely.

The absorbance in units ε Cl can directly be related to the 1/e or ring-down time of the measured decays via:

$$\varepsilon C_{\text{eff}} l = \frac{\alpha_{\text{anal}} l}{2.303} = \frac{n_{\text{avg}} L}{2.303 c}\left[\frac{1}{\tau} - \frac{1}{\tau_0}\right] \quad (1)$$

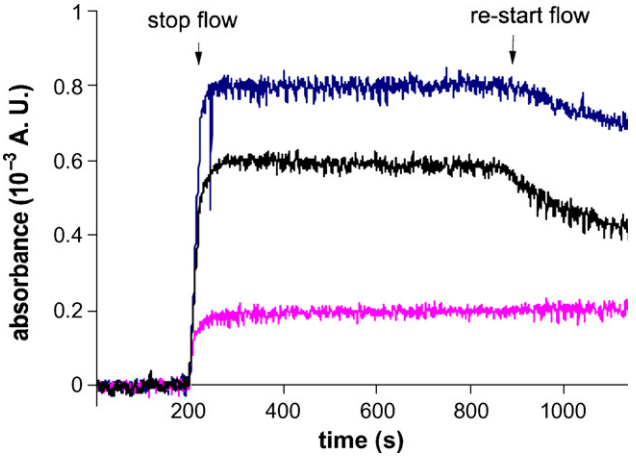

Fig. 3. Flow profiles on the different surfaces; cyt *c* concentration: 10 μM. From top to bottom: the bare silica surface, the NH_2-coated surface and the C_{18}-coated surface.

where ε is the molar extinction coefficient in $M^{-1}\,cm^{-1}$ at 538 nm, C_{eff} the effective concentration in the penetration layer in M and l the effective path-length of the evanescent wave through the sample in cm. L is the cavity length (71–73 mm in this study), n_{avg} the average refractive index, c the speed of light, and α_{anal} is the absorption coefficient in cm^{-1}; τ and τ_0 are the ring-down times in presence or absence of analyte.

The evanescent waves emanating from a surface exhibit an exponentially decaying field intensity along the spatial coordinate perpendicular to the surface; different from a propagating wave an evanescent wave exhibits a field amplitude in all three spatial dimensions, E_x, E_y, and E_z. The effective depth d_e of the EW is defined as the path-length in a conventional transmission geometry that when inserted in the Lambert–Beer law would result in the same degree of absorbance. For p-polarized (in the plane of the beam and the surface normal) light, this d_e can be calculated according to [22]:

$$d_e = \frac{n_{21}\lambda(2\,\sin^2\theta - n_{21}^2)\cos\theta}{n_1\pi(1-n_{21}^2)[(1+n_{21}^2)\sin^2\theta - n_{21}^2]\sqrt{\sin^2\theta - n_{21}^2}} \quad (2)$$

where θ is the angle of incidence (70° in our case), λ the wavelength of the light (538 nm) and n_1 and n_2 are the refractive indices of fused silica (1.46) and the liquid medium (1.33), respectively, and $n_{21} = n_2/n_1$.

Equation (2) specifically holds for a situation in which a bulk sample is probed near a surface. The presently calculated effective depth of 1100 nm is much larger than that of the previous set-up (400 nm) due to a difference in reflection angle at the TIR surface and the refractive index of the prism material [12]. This can also be considered as a rough measure of the distance and the volume of the bulk over which detection takes place near the surface, although the relationship between a penetration depth d_p and the effective depth d_e is nontrivial and has led to confusion [23]. For *p*-polarization the effective depth d_e is found to be larger than for the case of *s*-polarization and is also much larger than d_p for our set-up; in our case $n_{21} = 0.91$.

An intriguing characteristic of evanescent waves, as exploited in total internal reflection (TIR) and attenuated total reflection (ATR) spectroscopies, and now also in evanescent-wave CRDS, is that the absorbance close to the surface is strongly enhanced. For a thin layer with thickness d ($d \ll d_e$) the effective depth due to absorption by this layer for *p*-polarization is calculated [23]:

$$\frac{4n_{t1}d\,\cos\theta[(1+n_{2t}^4)\sin^2\theta - n_{21}^2]}{(1-n_{21}^2)[(1+n_{21}^2)\sin^2\theta - n_{21}^2]} \quad (3)$$

Inserting the values for the angle of incidence θ, the indices of refraction ($n_{ij} = n_i/n_j$), and n_t referring to the thin layer ($n_t = 1.35$), the resulting value for d_e is much larger than d, the thickness of the cyt *c* layer (ca. 3–3.5 nm). This gives rise to an enhancement factor $\eta = d_e/d$ of 8.3 for the presently chosen experimental conditions. This factor is largely due to a strong electromagnetic intensity of the EW along the *z*-coordinate.

An isotherm (shown in Fig. 4) was measured and the data were fitted to

$$A = \frac{A_{\max} K C_{\text{eq}}}{1 + K C_{\text{eq}}} \quad (4)$$

where A is the measured absorbance, $A_{\max}$ the absorbance that would be measured at maximum coverage (both in AU and corrected for the bulk absorbance for a effective depth of 1100 nm), K the equilibrium constant for the adsorption (in μM^{-1}) and C_{eq} is the equilibrium concentration in the bulk (in μM), which given the concentrations and volumes applied was taken as equal to the initial (injected) concentration. Parameters obtained from the

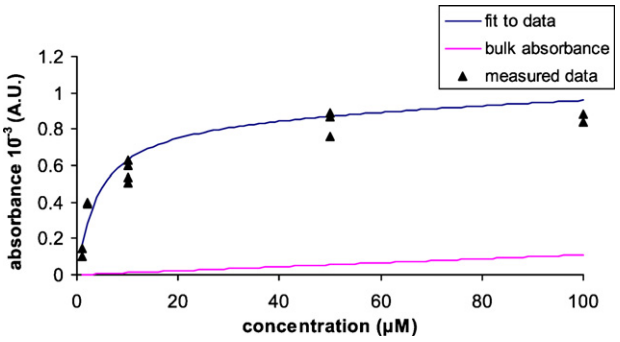

Fig. 4. Average of three cyt *c* adsorption isotherms as measured on the bare SiOH surface, together with a fit to the data (regression coefficient 0.97). The straight line indicates the calculated bulk (background) absorbance using an effective penetration depth of 1100 nm. Data points were measured on different days using fresh solutions.

fits were: $A_{max} = (8.9 \pm 2) \times 10^{-4}$ AU, $K = (23 \pm 14) \times 10^4\ M^{-1}$ and $\Delta G = (30 \pm 2)$ kJ/mol. The average fit is included in Fig. 4. An important – and most likely incorrect – assumption for the fits was that there is only one kind of adsorption site available for the cyt *c* molecules. It is known that on a hydroxylated SiOH surface, two different silanol sites (the so-called Q2 and Q3 sites) exist and therefore two different adsorption sites should be taken into account [24,25]. Furthermore, additional multi-layer adsorption may take place so that we are dealing with a multitude of adsorption sites: the surface and the different cyt *c* layers. Cyt *c* is not a hard, positive sphere, but rather a large molecule with a net charge of +11 at pH 7.4; negative charges as well as positive charges are present on the protein surface. Since the positive charges are mainly located in one specific region of the surface which will be pointing towards a negative surface when adsorbed, these negatively charged regions are pointing towards the bulk solution providing possible adsorption sites. In addition, it must be noted that the cyt *c* adsorption is partially irreversible indicating that equilibrium is not reached. Presumably, the Langmuir adsorption model will not adequately describe the measured data.

It is illustrative to estimate the absorbance which would be measured for a complete cyt *c* monolayer. From the cyt *c* dimensions it is estimated that in a cyt *c* monolayer with thickness of 3–3.5 nm, (0.6–0.7) $\times 10^{12}$ molecules or 1–1.2 pmol are present in the laser spot (estimated to be 6–7 mm^2). Previously, monolayer coverage of 32 pmol/cm^2 amounting to 1.9 pmol in 6–7 mm^2 was measured with electrochemical techniques [26], quite close to the present estimation. Using the cyt *c* extinction coefficient of $1.0 \times 10^4\ M^{-1}\ cm^{-1}$ at 538 nm , the absorbance of a monolayer (15–18 pmol/cm^2) should be (1.5–1.8) $\times 10^{-4}$ AU in a conventional transmission geometry. However, when applied to thin films ($d \ll d_e$) the enhancement factor comes into play, which is calculated to be $\eta = 8.3$ for the present experimental conditions (see above). Therefore, the EW absorbance is expected to be 12×10^{-4} to 15×10^{-4} AU Thus, the experimental results (maximum absorbance of $8.9 \pm 2 \times 10^{-4}$ AU) indicate that the maximum coverage observed on the three surfaces is close to a monolayer. An assumption in this estimation is that the extinction coefficient of the adsorbed cyt *c* is the same as for bulk (randomly oriented) molecules. This seems unlikely since, at least in the case of electrostatic adsorption, cyt *c* is known to be adsorbed with its heme group almost perpendicular to the surface [27]. The transition dipole moments of the two Q-bands lie in the plane of the heme [28]; the band at 538 nm corresponds to the transition dipole moment perpendicular to the surface, the extinction coefficient is expected to be higher than measured in bulk.

3.2. Cytochrome c adsorption to modified surfaces

A future application of EW-CRDS is the development of a biosensor. Such a device requires the immobilization of a protein, an antibody or another biomolecule in order to monitor its interactions with analytes in the liquid mobile phase. Ideally, the biosensor will only exhibit specific interactions while non-specific binding of analytes is minimal. Of course, in EW-CRDS the crucial point is whether such an immobilization deteriorates the reflection quality of the TIR surface or not. To make EW-CRDS feasible the surface of the prism has to be modified in such a way that the measured ring-down signal is not strongly shortened with respect to the original signal measured on a bare prism. Various possibilities exist for the immobilization of proteins and antibodies on a silica surface. For example, one can add SH-groups to the "tail" of an IgG antibody in order to link the antibodies to a maleimide-activated NH_2-coated surface. Another possibility is using the non-specific binding on a hydrophobic surface (for example, C_{18}-coated surface); the disadvantage of this approach is that the active region of some of the immobilized antibodies may not be accessible for the antigen (analyte) anymore.

Previously, we determined that surface roughness (possibly induced by an imperfect layer on the surface) is not a serious problem: when using an EW-CRDS configuration with an intra-cavity prism, most optical losses will occur at the entrance and exit face of the prism rather than from scattering at the TIR surface. As reported earlier, higher surface roughness appeared to be advantageous for analytical purposes, presumably because imperfect flow results in more efficient exchange between the analytes of interest and the surface: the flow was estimated to be turbulent based on calculation of the Reynolds number for this particular system [12].

In the present study we demonstrate a user-friendly one-step protocol for attaching the C_{18} or NH_2-layer. Again, cyt *c* was chosen as a test molecule. In Fig. 3, it is immediately seen that at the 10- μM level the adsorption on bare silica is about 2 to 4 times higher than on the coated surfaces. In view of the development of a biosensor this is a rather encouraging result, since a-specific binding is successfully being suppressed. On the C_{18} surface, the flow profile shows no gradual decrease after re-starting the flow indicating that cyt *c* is irreversibly attached to this layer. Such an irreversible binding is not unexpected since the aliphatic chains on the surface are known to denature the protein. The NH_2-surface should be positively charged at the used pH 7.4 and is therefore expected to repel cyt *c*. The fact that also for this layer some adsorption can still be seen suggests that the bare silica surface is not completely shielded or covered by the NH_2-layer.

For all three surfaces cyt *c* adsorption is at least partly irreversible at the time-scale and under the conditions of the measurements. Contrary to the bare silica surface, cleaning of the coated surfaces after performing an adsorption experiment is not trivial. The original ring-down time as measured on the clean C_{18} and NH_2 surfaces is recovered after one night of flushing (at 2 ml/min) with pure methanol (C_{18}) or 1:1 methanol/water (NH_2). The nature of the interactions for the three surfaces will most probably be different. In the case of bare silica and NH_2-coated surface electrostatic interactions will be significant, whereas adsorption to the C_{18} surface will be dominated by hydrophobic interactions while electrostatic contributions will be small. Especially for the C_{18} surface, considerable irreversible binding should be expected, but flushing with abundant organic solvent (e.g. methanol) is sufficient for completely removing strongly bound cyt *c*. A prism that was used for months yielded the same results as a newly coated prism.

Finally, we tried to fit a Langmuir isotherm to the data points obtained for the NH_2- and C_{18}-coated surfaces, but this attempt was not successful. Presumably, the requirement of equilibrium

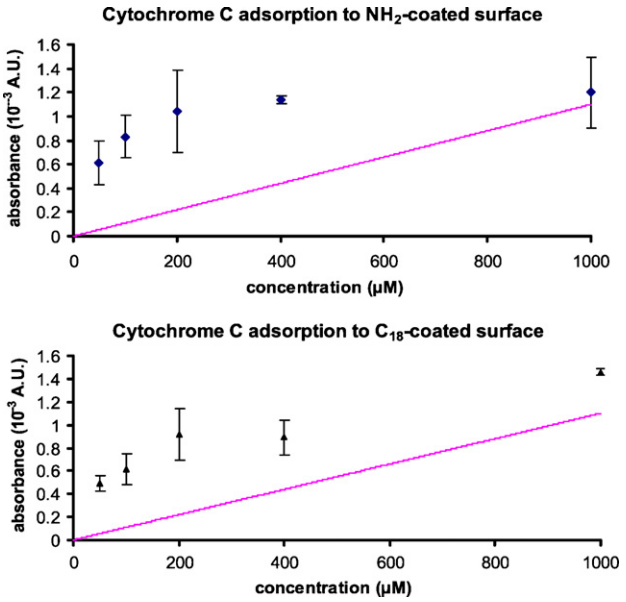

Fig. 5. Adsorption isotherms as measured on the C_{18} and NH_2 surfaces, measured in triplicate. The straight lines indicate the calculated bulk (background) absorbances using an effective penetration depth of 1100 nm. Data points were obtained on different days using fresh solutions.

conditions is not fullfilled; in the case of the C_{18}-layer the binding is even irreversible. The measured adsorption isotherms for the two surfaces are shown in Fig. 5. One may argue that a fit of the data to a simple Langmuir isotherm is not adequate for the determination of thermodynamic parameters such as a maximum coverage. A more appropriate model would take into account adsorption to three different adsorption sites (the surface, the first, oriented, cyt *c* monolayer and possibly also layers on top that are more randomly oriented). In the case of the C_{18} surface where adsorption will be due to hydrophobic rather than electrostatic interactions, only two sites should be taken into account since the first monolayer will probably not be oriented. However, it is clear that the affinity of cyt *c* is highest towards the bare silanol surface, followed by the NH_2-coated and the C_{18}-coated surfaces.

4. Conclusion

Surface modification of the TIR face of a prism used in EW-CRDS by self-assembly from solution has been demonstrated to be feasible. By means of surface modification, EW-CRDS could be developed into an interesting tool for sensitive absorbance spectroscopic studies of adsorption kinetics towards surfaces with different properties. In the present geometry reflection and scattering losses in the system are still high and are limiting further detection sensitivity improvements. It is expected that an improved design of the prism used for EW-CRDS, for example the use of a folded resonator [29], can drastically increase the sensitivity of the system. Finally it is noted that the current design involving normal-incidence entrance and exit faces would allow for polarization-dependent studies: in that case the orientation of the adsorbed molecule could be calculated from the dichroic ratio.

Acknowledgements

We wish to thank E. Zoethout and E. Louis at FOM institute for Plasma Physics at Rijnhuizen, the Netherlands for providing silicon wafers used for XPS measurements and performing the XPS analyses and data interpretation. This research is supported by a project grant (02PR2243) from the Netherlands Foundation for Fundamental Research of Matter (FOM).

References

[1] A.C.R. Pipino, J.W. Hudgens, R.E. Huie, Evanescent wave cavity ring-down spectroscopy with a total-internal-reflection minicavity, Rev. Sci. Instr. 68 (1997) 2978–2989.
[2] P. Claudon, M. Donner, J.F. Stoltz, Potential interest of optical fibers as immunosensors—study of different antigen coupling methods, J. Mater. Sci. Mater. Med. 2 (1991) 197–201.
[3] A. Klotz, A. Brecht, C. Barzen, G. Gauglitz, R.D. Harris, G.R. Quigley, J.S. Wilkinson, R.A. Abuknesha, Immunofluorescence sensor for water analysis, Sens. Actuators B 51 (1998) 181–187.
[4] D.S. Walker, H.W. Hellinga, S.S. Saavedra, W.M. Reichert, Integrated optical waveguide attenuated total reflection spectrometry and resonance Raman spectroscopy of adsorbed cytochrome c, J. Phys. Chem. 97 (1993) 10217–10222.
[5] R. Guidelli, G. Aloisi, L. Becucci, A. Dolfi, M.R. Moncelli, F.D. Buonsegni, New directions and challenges in electrochemistry—bioelectrochemistry at metal/water interfaces, J. Electroanal. Chem. 504 (2001) 1–28.
[6] P. Hildebrandt, M. Stockburger, SERRS of cytochrome c at room and low temperatures, J. Phys. Chem. 90 (1986) 6017–6024.
[7] P.L. Edmiston, J.E. Lee, S.-S. Cheng, S.S. Saavedra, Molecular orientation distributions in protein films. 1. Cytochrome c adsorbed to substrates of variable surface chemistry, J. Am. Chem. Soc. 119 (1997) 560–570.
[8] Z.-M. Qi, N. Matsuda, A. Takatsu, K. Kato, A kinetic study of cytochrome c adsorption to hydrophilic glass by broad-band, time-resolved optical waveguide spectroscopy, J. Phys. Chem. B 107 (2003) 6873–6875.
[9] W. Xu, H. Zhou, F.E. Regnier, Regio-specific adsorption of cytochrome c on negatively charged surfaces, Anal. Chem. 75 (2003) 1931–1940.
[10] Y.-Y. Cheng, S.H. Lin, H.-C. Chang, Probing adsorption, orientation and conformational changes of cytochrome c on fused silica surfaces with the Soret band, J. Phys. Chem. A 107 (2003) 10687–10694.
[11] C.M. Kraning, T.L. Benz, K.S. Bloome, G.C. Campanello, V.S. Fahrenbach, S.A. Mistry, C.A. Hedge, K.D. Clevenger, K.M. Gligorich, T.A. Hopkins, G.C. Hoops, S.B. Mendes, H.-C. Chang, M.-C. Su, Determination of surface coverage and orientation of reduced cytochrome c on a silica surface with polarized ATR spectroscopy, J. Phys. Chem. C 111 (2007) 13062–13067.
[12] L. van der Sneppen, J. Buijs, C. Gooijer, W. Ubachs, F. Ariese, Evanescent-wave cavity ring-down spectroscopy for enhanced detection of surface binding under flow injection analysis conditions, Appl. Spectrosc. 62 (2008) 649–654.
[13] R. Engeln, G. Berden, E. van den Berg, G. Meijer, Polarization dependent cavity ring down spectroscopy, J. Chem. Phys. 107 (1997) 4458–4467.
[14] F. Li, R.N. Zare, Molecular orientation study of methylene blue at an air/fused-silica interface using evanescent-wave cavity ring-down spectroscopy, J. Phys. Chem. B 109 (2005) 3330–3333.
[15] M.A. Everest, V.M. Black, A.S. Haehlen, G.A. Haveman, C.J. Kliewer, H.A. Neill, Hemoglobin adsorption to silica monitored with polarization-dependent evanescent-wave cavity ring-down spectroscopy, J. Phys. Chem. B 110 (2006) 19461–19468.
[16] J.J. Cras, C.A. Rowe-Taitt, D.A. Nivens, F.S. Ligler, Comparison of chemical cleaning methods of glass in preparation for silanization, Biosens. Bioelectr. 14 (1999) 683–688.
[17] P. Silberzan, L. Leger, D. Ausseree, J.J. Benattar, Silanation of silica surfaces. A new method of constructing pure or mixed monolayers, Langmuir 7 (1991) 1647–1651.
[18] M.E. McGovern, K.M.R. Kallury, M. Thompson, Role of solvent on the silanization of glass with octadecyltrichlorosilane, Langmuir 10 (1994) 3607–3614.
[19] J.R. Shallenberger, E. Metwalli, C.G. Pantano, F.N. Tuller, D.F. Fry, Adsorption of polyamides ond polyamide-silane mixtures at glass surfaces, Surf. Interf. Anal. 35 (2003) 667–672.
[20] J.H. Scofield, Hartree-Slater subshell photoionization cross-sections at 1254 and 1487ev, J. Electron Spectrosc. Related Phenom. 8 (1976) 129–137.
[21] S.K. Chan, I. Tulloss, E. Margoliash, Primary structure of the cytochrome c from the snapping turtle, chelydra serpentina, Biochemistry 5 (1966) 2586–2597.
[22] N.J. Harrick, Infrared Reflection Spectroscopy, Harrick Scientific Corporation, New York, USA, 1987.
[23] F.M. Mirabella, Principles, Theory and Practice of Internal Reflection Spectroscopy: in J.M. Chalmers, P.R. Griffiths (eds.) Handbook of Vibrational Spectroscopy, Vol 2., Wiley, Chichester, UK, 2002.
[24] A.M. Shaw, T.E. Hannon, F. Li, R.N. Zare, Adsorption of crystal violet to the silica–water interface monitored by evanescent wave cavity ring-down spectroscopy, J. Phys. Chem. B 107 (2003) 7070–7075.
[25] H.-F. Fan, F. Li, R.N. Zare, K.-C. Lin, Characterization of two types of silanol groups on fused-silica surfaces using evanescent-wave cavity ring-down spectroscopy, Anal. Chem. 79 (2007) 3654–3661.
[26] R.A. Clark, E.F. Bowden, Voltammetric peak broadening for cytochrome c/alkanethiolate monolayer structures: dispersion of formal potentials, Langmuir 13 (1997) 559–565.
[27] W.H. Koppenol, E. Margoliash, The asymmetric distribution of charges on the surface of horse cytochrome c, J. Biol. Chem. 257 (1981) 4426–4437.
[28] J.G.E.M. Fraaije, J.M. Kleijn, M. van der Graaf, J.C. Dijt, Orientation of adsorbed cytochrome c as a function of the electrical potential of the interface studied by total internal reflection fluorescence, Biophys. J. 57 (1990) 965–975.

[29] A.C.R. Pipino, Ultrasensitive surface spectroscopy with a miniature optical resonator, Phys. Rev. Lett. 83 (1999) 3093–3096.

Biographies

L. van der Sneppen(born 7th of January 1981) obtained her PhD from the Vrije Universiteit Amsterdam on 10th of November 2008. She received a Rubicon grant from the Netherlands Foundation for Scientific Research (NWO) for her current research at the University of Oxford, United Kingdom. She will continue the current research using different measurement principles as well as develop fiber-based trace gas-sensors.

C. Gooijer is Full Professor and head of the Applied Spectroscopy group of the Laser Centre of the Vrije Universiteit Amsterdam. He is an enthusiastic lecturer and is involved in analytical chemistry and physical chemistry oriented research, specifically spectroscopic detection and identification methods for analytical separation methods, high-resolution luminescence, time-resolved luminescence and Raman spectroscopy.

W. Ubachs obtained a PhD degree from Nijmegen University and is currently Professor of Atomic, Molecular and Laser Physics at VU University Amsterdam, as well as Director of the Laser Centre VU. His interests are in high resolution spectroscopy, non-linear optics, and optical techniques for chemical sensing.

F. Ariese obtained his PhD at the Vrije Universiteit Amsterdam in 1993 for his research on cryogenic fluorescence techniques. He then worked as a postdoc at Iowa State University (USA) and at the Institute for Environmental Studies/VU-IVM. He is currently associate professor in the Applied Spectroscopy group of the Laser Centre VU. His main research interest is the development of new analytical applications for fluorescence, phosphorescence, Raman spectroscopy, cavity ring-down spectroscopy, and the coupling of these techniques to separations.